

David C. Miller<sup>1\*</sup>, Michael D. Kempe<sup>1</sup>, Kenji Araki<sup>2</sup>, Cheryl E. Kennedy<sup>1</sup>, and Sarah R. Kurtz<sup>1</sup>

\*David.Miller@nrel.gov

<sup>1</sup> National Renewable Energy Laboratory (NREL), 1617 Cole Blvd., Golden, CO, USA 80401  
[http://www.nrel.gov/pv/performance\\_reliability/](http://www.nrel.gov/pv/performance_reliability/)

<sup>2</sup> Daido Steel Co., Ltd. 2-30 Daido-cho, Minami, Nagoya 457-8545, Japan

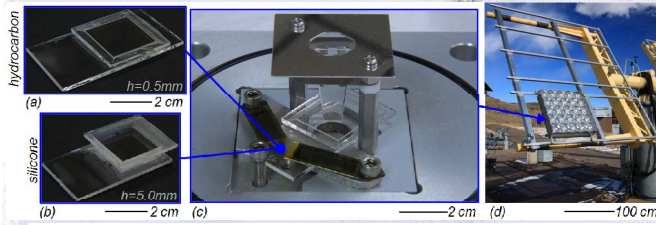
Presented at the PV Module Reliability Workshop, February 16-17, 2011, Golden, Colorado

## Introduction

**Polymeric encapsulation materials** are typically used in concentrating photovoltaic (CPV) modules to protect the cell from the field environment. Because it is physically located adjacent to the cell, the encapsulation is exposed to a high optical flux, often including light in the ultraviolet (UV) and infrared (IR) wavelengths. The durability of encapsulants used in CPV modules is critical to the technology, but is presently not well understood. This work seeks to identify the appropriate material types, field-induced failure mechanisms, and factors of influence (if possible) of polymeric encapsulation. These results will ultimately be weighed against those of future qualification and accelerated life test procedures.

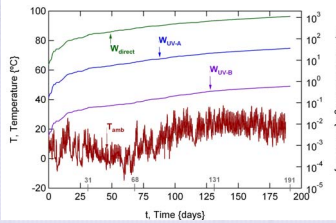
## Background

**Test specimens**, including: ethylene-co-vinyl acetate (EVA), polyvinyl butyral (PVB), poly(ethylene-co-methacrylic acid metal salt) (ionomer), polyethylene and polyoctene copolymer ("polyolefin", PO), thermoplastic polyurethane (TPU), poly(dimethylsiloxane) (PDMS), and poly(phenyl-methyl silane) (PPMS) were formed between quartz slides. Some of the test materials come from the existing flat-panel PV field and were not specifically formulated for use in CPV. Hydrocarbon formulations often contain a UV stabilization system whereas the silicones typically do not. Hydrocarbon-based materials were laminated to be 0.5-mm thick (as popular in existing film products) whereas silicones were molded to be 5.0-mm thick (to distinguish between these exceptionally optically transmitting materials). Specimens were situated between a secondary optic and then inserted in a contemporary CPV module product (nominally 500x concentration). The module uses a domed Fresnel lens as its primary optical element, and is mounted on a tracker in Golden, CO. Measurements (including hemispherical transmittance, direct transmittance, mass loss, and visual appearance) were performed periodically (0, 1, 2, 4, 6, 12, 18, 24, 30, 36 ... months). The initial results (for 6 months cumulative aging in the field) are summarized here.



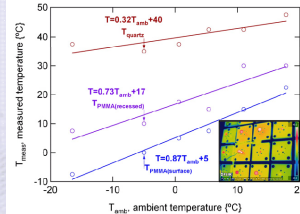
ABOVE: Photographs of representative (a) hydrocarbon and (b) silicone test specimens, are inserted (c) behind a secondary optic element and then (d) into a CPV module. The tracker-mounted module can accommodate 25 separate specimens (no duplicate formulations are used here).

**Environmental conditions** at the test site are logged using a plethora of instruments, including module-located thermocouples. Instruments not immediately present at the Outdoor Test Facility (OTF) are supplemented by those at the Solar Radiation Research Laboratory (SRRL), located on top of South Table Mountain.



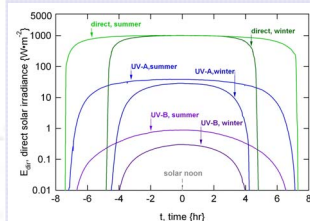
LEFT: Temperature and dose data from the OTF. The maximum and minimum temperatures of 36°C and -15°C, respectively, were observed during the first 6 months in the field. The damaging dose of solar radiation (note logarithmic scale) is distinguished here between "UV-B" (from 280-320 nm), "UV-A" (320-400 nm), and "direct" (285-2900 nm) wavelengths. Seasonal (winter) cloudiness is evident in the lesser slope during the first month relative to that encountered during the sunny summer months (the latter half of the data). The raw dose of radiation incident on first surface of the lens is shown in the figure. The dose at the encapsulation may be analyzed from the measured transmittance of the CPV optical system; its damaging effect may be further understood using the specimen's action spectrum.

**Specimen temperature** was determined using infrared thermography. For the purpose of the work here, it is critical that the specimen temperature be representative of CPV module products. For example, excessive temperature (because the cell and heat sink are not present) may motivate spurious failure modes.



RIGHT: The temperature of the quartz substrate is shown relative to that of the ambient and the poly(methyl methacrylate) (PMMA) lens. A thermal image of the back of the module is shown in the inset. From the thermal rise for the quartz (+40°C), the existing data suggests the specimen temperature of 75°C during the hottest summer days (36°C). The data for the lens indicates that its surface is cooler than the sites where it is attached to the module. A more advanced model may be used to account for the solar irradiance and wind.

**The direct solar resource** at the test site (elevation of 1.79 km) includes greater UV radiation than that found at other locations. Furthermore, the steppe climate typically features at least 300 half-days of sunshine. Seasonal differences between the duration and magnitude of the solar radiation, however, do arise based on the site location (latitude of 39.740 °N). A 4.2x, 2.3x, and 1.6x difference exists between the raw dose (integral) of radiation present during the summer and winter months based on duration, for the UV-B, UV-A, and direct wavebands, respectively. Another 2.9x, 1.3x, and 1.0x difference exists between the magnitude of radiation present during the summer and winter months based on magnitude, for the UV-B, UV-A, and direct wavebands, respectively. The damaging dose of UV-B radiation (which scales with both duration and magnitude) is therefore at least 10x greater in the summer months. For polymeric materials, radiation induced damage may be coupled to the temperature, further complicating seasonal differences.



ABOVE: Irradiance data (note logarithmic scale), measured on cloudless days at the OTF. The differences in the duration and magnitude of radiation present are readily distinguished in the figure.

## Acknowledgements

The authors are grateful to: Dr. Keith Emery, Mr. Matt Muller, Dr. Daryl Myers, Dr. John Pern, Matt Beach, Christa Loux, Tom Moricone, Marc Oddo, Bryan Price, Kent Terwilliger, and Robert Tirawat of the National Renewable Energy Laboratory for their discussion/help with the solar spectrum, experimental methods, and optical measurements, respectively. The authors would also like to thank Mr. Gargagnon of Bixby International Corp. for participation and help with specimens and related understanding. This work was supported by the U.S. Department of Energy under Contract No. DE-AC36-08GO28308 with the National Renewable Energy Laboratory.

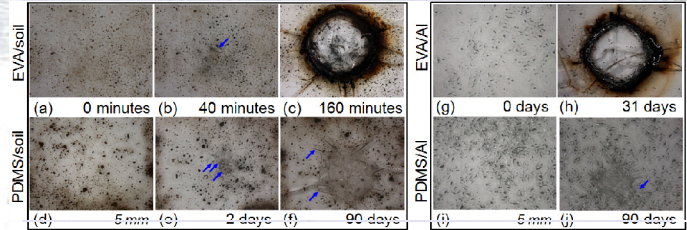
## For More Information,

refer to the publications:  
 D.C. Miller, M.D. Kempe, C.E. Kennedy, S.R. Kurtz, "Analysis of Transmitted Optical Spectrum Enabling Accelerated Testing of Multi-Junction CPV Designs", *Optical Engineering*, 50 (1), 2010, 013003.  
 D.C. Miller, M.D. Kempe, K. Araki, C.E. Kennedy, S.R. Kurtz, "The Durability of Polymeric Encapsulation Materials for Concentrating Photovoltaic Systems", Proceedings of the 7th International Conference on Concentrating Photovoltaic Systems (Las Vegas, Nevada), 2011.

## Experimental Results

**Discovery experiments** using EVA and PDMS specimens were conducted to become familiar with the CPV environment and to understand the effect of contamination embedded in the specimens. Catastrophic failure (thermal runaway followed by material decomposition) may be quickly observed (within minutes or days) in CPV modules (geometric concentration ≥ 500x), if no homogenizing optic is used. The optical concentration at localized sites within the focus of a single optical element can easily be 1-3 orders of magnitude greater than the nominal geometric concentration. Such localized hot points are believed to have facilitated the destruction of EVA and PDMS specimens.

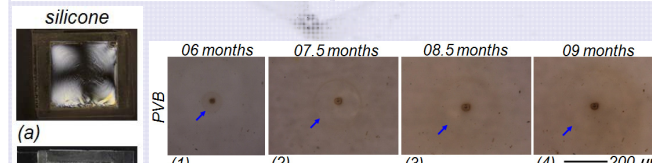
Soil, aluminum filings, polymer filings (black polyethylene), and voids (bubbles) were intentionally added to separate sets of EVA and PDMS specimens. Soil, aluminum, and polyethylene (PE) facilitated the thermal decomposition of EVA within 2, 31, and 2 days respectively. Like the earlier specimens, indicators of significant stress (including voided regions, localized delamination, and cracked glass) were observed in failed specimens. Only PE facilitated the thermal decomposition of PDMS; however, the soil and aluminum filled specimens became cracked within 2 days in the field. No primer was applied to the contamination, which may have facilitated the cracks in the PDMS. While voids reduce the optical transmittance, the specimens with bubbles did not appear changed after 116 consecutive days in the field.



ABOVE: The visual appearance of soil-contaminated EVA [(a)-(c)], soil-contaminated PDMS [(d)-(f)], aluminum-contaminated EVA [(g) & (h)], and aluminum-contaminated PDMS [(i) & (j)]. Discoloration and voiding (arrow) are evident in (b). The failed EVA specimens contain a voided central region, surrounded by charred, decomposed, and degraded material [(g) and (h)]. The PDMS was prone to cohesive failure (crack formation, [arrows in (e), (f), and (l)]).

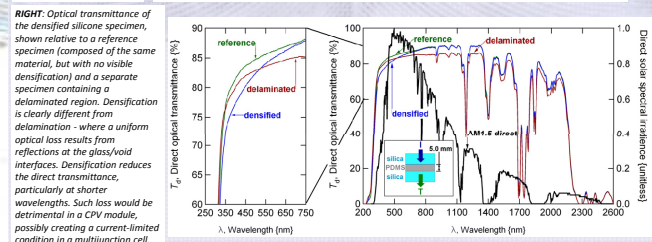
**The formal experiment** is presently examining (6) EVA, (2) PVB, (2) Ionomer, (1) PO, (1) TPU, (11) PDMS, and (2) PPMS specimens. A queue of candidates exists to follow any failed specimens.

RIGHT: The square outline of the homogenizer is clearly evident in an EVA specimen. The discovery experiment in (a) used a custom UV-transmitting test fixture (nominal concentration of 500x). Similar behavior is anticipated in the formal experiment for a PVB specimen (b). The locally degraded region near the center of the concentrated spot appears similar to those seen to precede failure in the discovery experiments.



ABOVE: The evolution of the PVB specimen from the formal study over time (1)-(4), as photographed using a microscope with fixed magnification steps. After the degraded region was observed at 6 months (1), the radius of an affected region (indicated with an arrow) is seen to increase in size, even during the cold winter months. Furthermore, separate affected regions (located adjacent to the original region) are becoming evident with time. Damage here is thought to be aided by thermal runaway of the degraded region, based on the increased optical absorbance of chromophore species.

LEFT: Observations of silicone specimens including: (a) desulfation, (b) cracking, and (c) haze formation. The desulfation in (a) was photographed using the method of cross-polarization. The lack of mass loss with time suggests the desulfation observed in 5 of the silicone specimens occurred during their molding. The fracture in the harder PDMS resin in (b) occurred during a period of cold weather (when the material is least compliant and least tough). Additional cracks have formed only during subsequent cold winter weather (not shown), suggesting the influence of thermal misfit stress. The outline of the homogenizer is evident in (c). Here, the degradation is attributed to its unique formulation.



**Future work** is planned to include chemical (FTIR, RAMAN, XPS, NMR) and polymer [differential scanning calorimetry (DSC)] analysis techniques. Traditional indicators (such as yellowness index) lack early warning (or predictive) capability, particularly in the case of thermal runaway. It is hoped that other methods (such as fluorescence spectrometry or chemical analysis) can provide predictive capability as well as insight into the mechanisms of degradation. Once a sufficient knowledge base is generated (including NREL's outdoor data as well as that shared by CPV researchers), NREL will work towards the development of indoor accelerated test methods. We hope to incorporate such methods into the CPV qualification standard(s) and use them to predict material lifetime in the field.

## Summary

The durability of polymeric encapsulation materials is being examined for the CPV application, using test coupons under the optics of a CPV module product. An assortment of popular encapsulants is presently under study. The monitoring of field conditions and diagnosis of specimen test conditions is essential to the work here. Discovery experiments identified the importance of optical flux uniformity and control of contamination. The initial field failures observed during the formal experiment include thermal decomposition (facilitated by thermal runaway), fracture (facilitated by thermal misfit), and haze formation (facilitated by the formulation chemistry). The work here will ultimately be applied towards test standards and lifetime prediction.